Trap-door optical buffering using a flat-top coupled microring filter: the superluminal cavity approach

Jacob Scheuer[1,2,*] and M. S. Shahriar[2,3]

[1]*School of Electrical Engineering, Tel-Aviv University, Tel-Aviv 69978, Israel*

[2]*Department of Electrical Engineering and Computer Science, Northwestern University, Evanston, Illinois 60208, USA*

[3]*Department of Physics, Northwestern University, Evanston, Illinois 60208, USA*

**Corresponding author: kobys@eng.tau.ac.il*

Received July 30, 2013; revised August 11, 2013; accepted August 12, 2013;
posted August 12, 2013 (Doc. ID 194701); published September 5, 2013

We propose and analyze theoretically a trap-door optical buffer based on a coupled microrings flat-top add/drop filter (ADF). By tuning one of the microrings into and out of resonance we can effectively open and close the buffer trap door and, consequently, trap and release optical pulses. To attain a maximally flat filter we present a new design approach utilizing the concept of a white light cavity to attain an ADF that resonates over a wide spectral band. We show that the resulting ADF exhibits superior performance in terms of bandwidth and flatness compared to previous design approaches. We also present a realistic silicon-on-insulator-based design and a performance analysis, taking into consideration the realistic properties and limitations of the materials and the fabrication process, leading to delays exceeding 5 ns for an 80 GHz bandwidth and a corresponding delay–bandwidth product of approximately 400. © 2013 Optical Society of America

OCIS codes: (120.2440) Filters; (200.4490) Optical buffers; (230.4555) Coupled resonators.
http://dx.doi.org/10.1364/OL.38.003534

Controlling the speed at which light propagates has been the focus of numerous studies during the past two decades [1]. In addition to the fundamental importance of the speed of light, the ability to control it opens up new avenues for diverse applications in telecommunications, nonlinear optics, sensing, and more [1]. In particular, the realization of optical delay lines and buffers by slowing down the speed of light has been explored thoroughly, primarily because such devices are key components for future all-optical networks. Slow light can be attained by utilizing atomic or photonic resonances [1]. Although the atomic-resonance-based devices provide slower light, it is the photonic structures that are more suitable for integration into practical systems. Consequently, numerous photonic slow-light structures, such as photonic crystal waveguides, coupled resonator optical waveguides, and many more, have been studied theoretically and experimentally [1,2]. Nonlinear effects such as Brillouin and Raman scattering [3–7] and coherent population inversion in semiconductor materials [8,9] have also been proposed and studied for slow-light and buffering applications.

Despite the inherent differences among these approaches, they all suffer from fundamental limitations in their ability to provide long delays of short pulses [10–12]. These limitations are often presented by the delay–bandwidth product (DBP) of a delay line, which serves as a figure of merit. Indeed, most slow-light-based delay lines exhibit DBPs that are of the order of unity. This rather inherent limitation inspired studies utilizing dynamic approaches to trap and release optical pulses [13–17]. Among these approaches, the most practical one is probably the "trap-door" buffer [14,15], a version of which has also been demonstrated experimentally [15]. The trap-door buffer concept (see, e.g., Fig. 1) utilizes an optical cavity that can be tuned between two states: "Open" and "Closed." In the Open state, the cavity is essentially transparent, allowing an optical pulse to enter. In the Closed state the cavity is opaque and prevents an optical pulse from either entering or exiting. Trapping a pulse is accomplished by setting the trap to the Open state, allowing the pulse to enter the cavity. Once inside, the trap is switched to the Closed state, thus trapping the pulse. To release the pulse, the trap is set to the Open state again, allowing the pulse to exit.

To attain large delays, it is essential to reduce the cavity round-trip losses as much as possible and to extend the cavity bandwidth while eliminating undesired dispersion effects. The utilization of microring resonators in the buffer concept presented in [15,18] introduces bandwidth limitations as well as dispersion effects due to the properties of the microring's spectral response. In [14,18] the use of white-light-cavity (WLC)-based mirrors was proposed to attain a larger bandwidth. Nevertheless, a practical realization of this concept using conventional

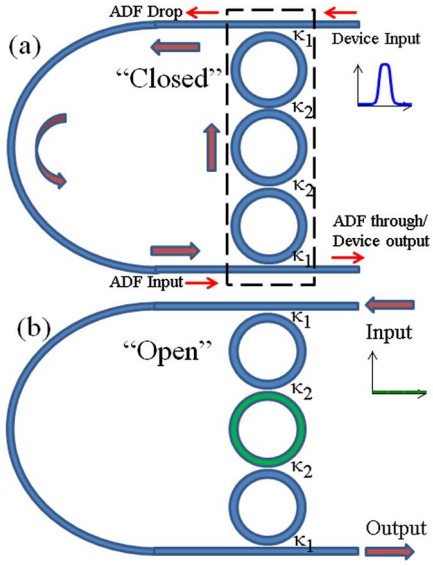

Fig. 1. Trap-door buffer: (a) Closed state, (b) Open state. AFD: add/drop filter.

systems such as fiber cavities and Brillouin gain peaks has proved to be very difficult to realize [19,20].

The key element in trap-door buffers is the design of the trap-door cavity mirror, which must provide a wide and flat reflectivity that is close to unity. In this Letter we propose and analyze a trap-door buffer utilizing a tunable coupled-resonator-based reflector. We focus primarily on the optimized design of the buffer reflector, attempting to achieve the widest and flattest spectral response possible. Figure 1 illustrates the concept of the proposed buffer. It is a ring cavity incorporating a tunable reflector composed of three coupled microrings. In the Closed state all microrings are tuned to the same resonance wavelength, resulting in high transmission in the drop port of the add/drop filter (ADF, indicated by the dashed box), thus forming a closed loop. In the Open state the central microring is tuned to a different resonance, resulting in low transmission in the ADF drop port, thus forming an open loop. The resonance of the middle microring can be tuned by using various mechanisms, such as free-carrier injection [15,21] and the Kerr effect [17].

The critical part of this concept is the door, in particular, its bandwidth and dispersive properties. We need the three-microring add/drop filter (ADF) to exhibit low loss and a flat response. The design parameters that we can use are the coupling coefficients between the microrings and between the microrings and the waveguides (see Fig. 1). From symmetry considerations it is clear that the arrangement depicted in Fig. 1 necessitates only two different coupling coefficients. The problem of coupled resonator filter design has been studied by Little *et al.* [22], who presented an approach for obtaining standard filter responses based on adapting filter design theory to the optical domain. Although this approach can provide plausible results, it does not offer physical insight to the resulting design (i.e., the coupling coefficients), which is useful for optimization. Here, we propose a physics-oriented approach for the required flat-top ADF design that not only provides a clear explanation of the mechanism that forms the flat-top spectral response but also provides a design that outperforms the one presented in [22].

The starting point of the design is an ADF composed of a single microcavity as illustrated in Fig. 2(a). Although the microcavity implementation (e.g., photonic crystal cavity, microring resonator, etc.) is of less importance, we choose to illustrate our design concept by using microring resonators as a concrete example. The transmission function of the drop port of an ideal (lossless) microring resonator is given by [23]

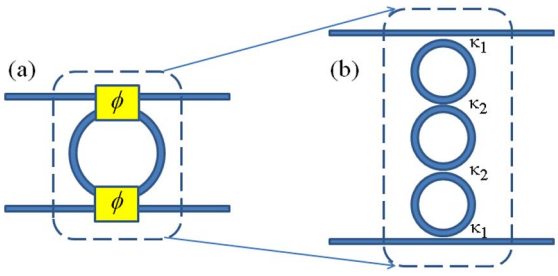

Fig. 2. WLC-based flat-top ADF comprising three cascaded microrings.

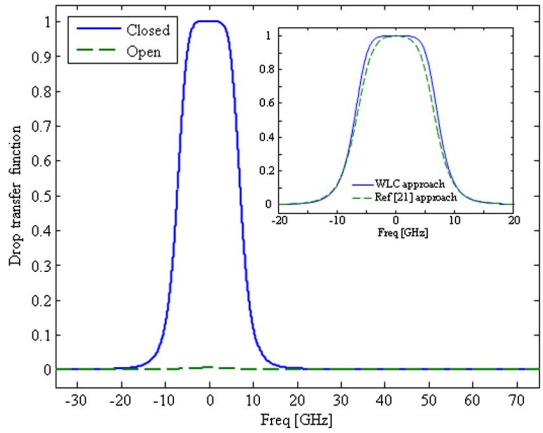

Fig. 3. Three-micoring ADF transmission function at the drop port for the Closed (solid blue) and the Open (dashed green) states. Inset, comparison between the drop transmission function of our design and that presented in [22].

$$D = \frac{-\sqrt{\kappa_1\kappa_2}\,\exp\left(\frac{1}{2}i\varphi\right)}{1-\sqrt{(1-\kappa_1)(1-\kappa_2)}\,\exp(i\varphi)}, \tag{1}$$

where $\kappa_{1,2}$ are the coupling coefficients between the microring and the I/O waveguides and φ is the frequency-dependent round-trip phase shift. If the two coupling coefficients are identical, the cavity is critically coupled and exhibits a 100% transmission at the drop port on cavity resonance [23]. Note that this 100% transmission exists only at the *resonances* of the microcavity. Let us assume that we have a cavity that resonates over a *continuous* spectral band (i.e., a WLC). As the transmission function of the filter is determined by the coupling coefficients (which are unchanged) and the round-trip phase, an ADF utilizing such a cavity will exhibit 100% drop efficiency over this spectral band, thus providing the desired flat-top response.

A WLC is characterized by the property that it resonates over a continuous spectral band [24,25]. Although ideally the bandwidth of such a cavity could be infinite, higher-order dispersion effects limit it. A WLC can be realized by incorporating a negative phase shift component into the optical path. This component is designed to compensate for the frequency dependence of the phase accumulated in the cavity round trip. Specifically, it can be shown that this phase component satisfies [26]

$$\left.\frac{d\theta}{d\omega}\right|_{\omega_{\mathrm{res}}} = -\frac{L'}{c_0}n_{\mathrm{wg}}, \tag{2}$$

where θ is the phase response of the phase shifter, L' is the round-trip length of the cavity, and n_{wg} is the group index of the waveguide. The most critical issue in a WLC is, of course, the realization of a phase component with the desired response. Such phase elements have been proposed and demonstrated by using vapor cells, which were optically pumped in a precise configuration [14,27], and by an intracavity resonator [26]. In the latter approach, a phase response satisfying Eq. (2) can be attained by properly setting the coupling coefficients of the intracavity resonator. Figure 2 illustrates the concept of

the design, comprising a microring resonator [serving as the main cavity of the ADF: Fig. 2(a)] and two couplers, which also provide the necessary phase shift. Each coupler and phase shifter is implemented by a microring resonator with coupling coefficients κ_1 and κ_2, thus forming a three-coupled-resonator structure.

Each external cavity serve as a phase shifter that compensates *half* the phase accumulated in each round trip in the middle ring (which is the main ADF cavity). Therefore, to attain the WLC condition, the coupling coefficients must satisfy [26]

$$\beta = \frac{1}{2\alpha}\left[1+\alpha^2+K(1-\alpha^2)-\sqrt{(1+\alpha^2+K[1-\alpha^2])^2-4\alpha^2}\right], \tag{3}$$

where $\alpha^2 = 1-\kappa_2$, $\beta^2 = 1-\kappa_1$, and K is the ratio between the round-trip length of the external cavities and the length of the normal propagation section that it is supposed to compensate for (in our case, half the round-trip length of the middle microring). If all the microrings have the same radius, then $K = 2$. Note that Eq. (3) only provides a relation between the coupling coefficients and that there are infinite possible coupling coefficient combinations that satisfy the WLC condition.

Figure 3 depicts the spectral drop functions of a three-ring cavity set to the two states described above, as calculated by the transfer matrix method [28]. The platform is assumed to be silicon-on-insulator (SOI) (effective index of ~3.0), the microrings radius is ~50 μm, and the central wavelength is 1550 nm. To switch states, the middle ring is tuned outside the phase compensation bandwidth. If we choose κ_2 to be, e.g., 0.01, then Eq. (3) yields $\kappa_1 = 0.247$. As shown in Fig. 3, the drop transmission in the Closed state is almost unity over a bandwidth of ~10 GHz while in the Open state this transmission is less than 0.5%. The inset of Fig. 3 compares the drop transmission in the Closed state of our design approach to that presented in [22]. Clearly, the design based on the WLC approach provides a broader and flatter transfer function. The reason for the improved line shape of our design is that it does not assume small coupling coefficients, as are implicitly assumed in the formalism presented in [22]. The power coupling coefficient of 0.25 used here cannot be considered small, and therefore the design rules of [22] are less accurate in this case. This point is further illustrated in Fig. 4. Note that in the limit of small coupling coefficients both approaches converge to an identical solution.

Next, we consider a realistic design of an optical buffer based on the concept presented in Fig. 1. To realize a distortionless buffer, the trap-door filter must be sufficiently wide to accommodate the bandwidth of the optical pulse. In addition, the loop waveguide must be sufficiently long to accommodate the complete temporal duration of the pulse. Figure 4 depicts the spectral drop functions of a three-ring cavity set to the Closed state. Again, the platform is assumed to be SOI; the microrings radius is, however, ~10 μm, and the central wavelength is 1550 nm. Using Eq. (3), choosing κ_2 to be 0.03 yields $\kappa_1 = 0.39$. For comparison, we show the spectral response of an ADF designed according to [22]. Clearly, the bandwidth of this filter is substantially narrower, and it does not exhibit a

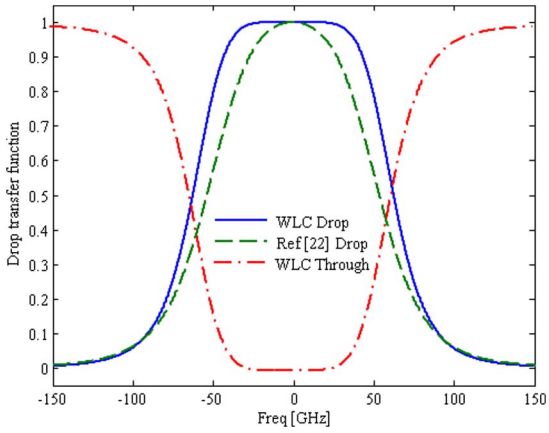

Fig. 4. Three-micoring ADF transmission function at the drop port for the Closed state: WLC-based design ($\kappa_2 = 0.03$; $\kappa_1 = 0.39$, solid blue), and design based on Ref. [22] ($\kappa_2 = 0.03$; $\kappa_1 = 0.49$, dashed green). Dashed–dotted red curve, through-port response of the WLC approach.

flat-top profile. The bandwidth of the WLC-based ADF exceeds 80 GHz, thus supporting pulses as short as 12.5 ps. The longitudinal extension of such a pulse in the silicon waveguide is ~1.1 mm. Thus we take the length of the loop to be 1.5 mm.

The primary mechanism limiting the buffering time or the attainable delay is the round-trip loss in the closed buffer. SOI-based waveguides with propagation losses of the order of 0.3 dB/cm have been demonstrated experimentally [29]. Thus a buffer round-trip loss of 0.06 dB (including filter losses) is feasible. The maximum attainable delay depends on the available signal-to-noise ratio. Assuming a signal-to-noise ratio of 20 dB [15] allows for 300 round trips in the buffer, yielding an overall delay of 5.1 ns and corresponding DBP of ~408. It is important to note that the dominant contribution to the buffer round-trip losses stems from the ADF employed. Increasing the coupling coefficients κ_1 and κ_2 reduces the overall finesse of the cavities (i.e., the number of revolutions in each microring), which affects the transmission properties of the ADF in two ways: increasing the usable bandwidth and reducing the loss [23]. Thus, increasing the coupling coefficients allows for not only shorter pulses but also lower losses and longer delays, thus further increasing the achievable DBP. On the other hand, large coupling coefficients would increase the transmission function of the ADF through port in the Open state and introduce distortions when the pulse enters and exits the device.

To explore further the performance and design tradeoffs of the buffer scheme, we consider a design for 30–52 ps pulses. The ADF is designed to accommodate the bandwidth of the shortest pulse, leading to $\kappa_2 = 0.002$ and $\kappa_1 = 0.12$, while the waveguide loop length is set according to the longest pulse, yielding $L_{\mathrm{Loop}} = 7.6$ mm. The radius of each microring is 10 μm, and the material system is SOI. Assuming a 20 dB maximal allowable attenuation, we find the maximal delay to be 2.7–2.85 ns, depending on the pulse duration. The dependence on the pulse duration is because the loss per round trip in the buffer is slightly larger for the shorter pulses owing to their wider bandwidths. Note

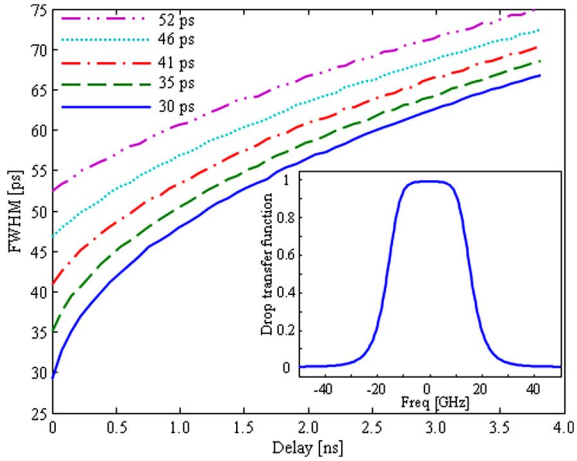

Fig. 5. Dependence of the pulse broadening in the buffer on the delay time for various pulse durations; Inset, drop port transmission function.

that for the 30 ps pulse the attainable delay is approximately 90 pulse durations.

Another important parameter to be considered is pulse broadening. Figure 5 depicts the FWHM of the pulse as a function of the delay. The inset shows the drop transmission function of the ADF. Clearly, the pulse broadens in the cavity, which necessitates regeneration, especially for the shorter pulses. This is because of the higher dispersion orders and losses of the ADF transmission, which have a greater impact on shorter pulses. Nevertheless, even the maximally broadened pulse does not exceed the length of the waveguide loop, which means that the round-trip loss is the dominant mechanism limiting the achievable delay.

In conclusion, we have proposed and analyzed a trapdoor buffer scheme that is capable of providing long delays for wide-bandwidth communication. The buffer design is based on a flat-top ADF comprising three coupled microring resonators, where the resonance frequency of the middle microring can be tuned to open and close the trap. To attain the maximal possible delay from the proposed scheme, we introduced a novel design approach for the ADF, which utilizes the concept of a white-light cavity in order to realize a maximally flat, wide-bandwidth response. We showed that this approach provides substantially larger bandwidth and flatness than those attained by previously reported approaches, especially beyond the weak coupling approximation.

Although the work presented here is focused on buffering applications, the design approach presented here is attractive for any application involving integrated optical filters and can be readily expanded to any number of coupled microcavities, thus providing a valuable tool for designing broadband flat-top filters. Nevertheless, for the specific application of optical buffering, increasing the number of cavities also increases the ADF transmission loss, thus limiting the DBP. Because the dominant mechanism limiting the attainable DBP is the round-trip loss (see Fig. 5), a three-cavity ADF design is a good compromise between the desired flat response and low transmission losses that facilitate long delay periods.

An SOI-based design, which accounts for the properties of the materials and leads to DBPs of the order of 400 have been presented. The proposed buffer has a 1.5 mm footprint and can be realized by using conventional deep-UV lithography and silicon processing methods, thus rendering it a practical component for optical delay and buffering applications.

The authors thank Alan Willner for useful comments and discussions. This work was supported in part by AFOSR under grant number FA9550-10-1-0228 and by the Israeli Science Foundation.

References

1. J. B. Khurgin and R. S. Tucker, *Slow Light: Science and Applications* (CRC Press, 2009).
2. J. Scheuer and M. Sumetsky, Laser Photon. Rev. **5**, 465 (2011).
3. J. Sharping, Y. Okawachi, and A. Gaeta, Opt. Express **13**, 6092 (2005).
4. D. Dahan and G. Eisenstein, Opt. Express **13**, 6234 (2005).
5. Y. Okawachi, M. S. Bigelow, J. E. Sharping, Z. Zhu, A. Schweinsberg, D. J. Gauthier, R. W. Boyd, and A. L. Gaeta, Phys. Rev. Lett. **94**, 153902 (2005).
6. K. Y. Song, M. G. Herráez, and L. Thévenaz, Opt. Express **13**, 82 (2005).
7. Z. Zhu, D. J. Gauthier, and R. W. Boyd, Science **318**, 1748 (2007).
8. M. S. Bigelow, N. N. Lepeshkin, and R. W. Boyd, Science **301**, 200 (2003).
9. C. J. Chang-Hasnain, P.-C. Ku, J. Kim, and S.-L. Chuang, Proc. IEEE **91**, 1184 (2003).
10. J. B. Khurgin, Opt. Lett. **32**, 133 (2007).
11. J. B. Khurgin, Opt. Lett. **31**, 948 (2006).
12. J. B. Khurgin, J. Opt. Soc. Am. B **22**, 1062 (2005).
13. M. F. Yanik and S. H. Fan, Phys. Rev. Lett. **92**, 083901 (2004).
14. H. Yum, X. Liu, Y. J. Jang, M. E. Kim, and S. M. Shahriar, J. Lightwave Technol. **29**, 2698 (2011).
15. Q. Xu, P. Dong, and M. Lipson, Nat. Phys. **3**, 406 (2007).
16. J. Scheuer, Europhys. Lett. **77**, 44004 (2007).
17. J. Scheuer, A. A. Sukhorukov, and Y. S. Kivshar, Opt. Lett. **35**, 3712 (2010).
18. H. N. Yum, M. E. Kim, Y. J. Jang, and M. S. Shahriar, Opt. Express **19**, 6705 (2011).
19. H. N. Yum, X. Liu, P. R. Hemmer, J. Scheuer, and M. S. Shahriar, Opt. Commun. **305**, 260 (2013).
20. H. N. Yum, J. Scheuer, M. Salit, P. R. Hemmer, and M. S. Shahriar, "Demonstration of white light cavity effect using stimulated Brillouin scattering in a fiber loop," arXiv:1307.5272v1 (2013).
21. Q. Xu, S. Manipatruni, B. Schmidt, J. Shakya, and M. Lipson, Opt. Express **15**, 430 (2007).
22. B. E. Little, S. T. Chu, H. A. Haus, J. Foresi, and J.-P. Laine, J. Lightwave Technol. **15**, 998 (1997).
23. A. Yariv and P. Yeh, *Photonics: Optical Electronics in Modern Communications*, 6th ed. (Oxford University, 2010).
24. R. H. Rinkleff and A. Wicht, Phys. Scr. **T118**, 85 (2005).
25. A. Rocco, A. Wicht, R.-H. Rinkleff, and K. Danzmann, Phys. Rev. A **66**, 053804 (2002).
26. O. Kotlicki, J. Scheuer, and M. S. Shahriar, Opt. Express **20**, 28234 (2012).
27. G. S. Pati, M. Salit, K. Salit, and M. S. Shahriar, Phys. Rev. Lett. **99**, 133601 (2007).
28. J. K. S. Poon, J. Scheuer, S. Mookherjea, G. T. Paloczi, Y. Huang, and A. Yariv, Opt. Express **12**, 90 (2004).
29. J. Cardenas, C. B. Poitras, J. T. Robinson, K. Preston, L. Chen, and M. Lipson, Opt. Express **17**, 4752 (2009).